ELEMENTA
Science of the Anthropocene

Assessing the O_2 budget under sea ice: An experimental and modelling approach

S. Moreau[1*] • H. Kaartokallio[2] • M. Vancoppenolle[3] • J. Zhou[4,5,6] • M. Kotovitch[5] • G. S. Dieckmann[7] • D.N. Thomas[2,8] • J.-L. Tison[5] • B. Delille[4]

[1]Georges Lemaître Centre for Earth and Climate Research, Earth and Life Institute, Université catholique de Louvain, Louvain-La-Neuve, Belgium
[2]Marine Research Centre, Finnish Environment Institute (SYKE), Helsinki, Finland
[3]Laboratoire d'Océanographie et du Climat, CNRS, Paris, France
[4]Unité d'océanographie Chimique, Université de Liège, Liège, Belgium
[5]Laboratoire de Glaciologie, Faculté des Sciences, Université Libre de Bruxelles, Bruxelles, Belgium
[6]Division of Earth and Ocean Sciences, Nicholas School of the Environment, Duke University, Durham, North Carolina, United States
[7]Alfred Wegener Institute for Polar and Marine Research, Bremerhaven, Germany
[8]School of Ocean Sciences, Bangor University, Menai Bridge, United Kingdom

*s.moreau@uclouvain.be

Abstract

The objective of this study was to assess the O_2 budget in the water under sea ice combining observations and modelling. Modelling was used to discriminate between physical processes, gas-specific transport (i.e., ice-atmosphere gas fluxes and gas bubble buoyancy) and bacterial respiration (BR) and to constrain bacterial growth efficiency (BGE). A module describing the changes of the under-ice water properties, due to brine rejection and temperature-dependent BR, was implemented in the one-dimensional halo-thermodynamic sea ice model LIM1D. Our results show that BR was the dominant biogeochemical driver of O_2 concentration in the water under ice (in a system without primary producers), followed by gas specific transport. The model suggests that the actual contribution of BR and gas specific transport to the change in seawater O_2 concentration was 37% during ice growth and 48% during melt. BGE in the water under sea ice, as retrieved from the simulated O_2 budget, was found to be between 0.4 and 0.5, which is in line with published BGE values for cold marine waters. Given the importance of BR to seawater O_2 in the present study, it can be assumed that bacteria contribute substantially to organic matter consumption and gas fluxes in ice-covered polar oceans. In addition, we propose a parameterization of polar marine bacterial respiration, based on the strong temperature dependence of bacterial respiration and the high growth efficiency observed here, for further biogeochemical ocean modelling applications, such as regional or large-scale Earth System models.

Domain Editor-in-Chief
Jody W. Deming, University of Washington

Associate Editor
Lisa A. Miller, Fisheries and Oceans Canada

Knowledge Domain
Ocean Science

Article Type
Research Article

Part of an *Elementa* Special Feature
Biogeochemical Exchange Processes at Sea-Ice Interfaces (BEPSII)

Received: May 29, 2015
Accepted: November 6, 2015
Published: December 3, 2015

Introduction

Bacteria play an important role in all marine systems, where they are fundamental for the remineralization of nutrients (e.g., Fripiat et al., 2014) and, therefore, regenerated production (i.e., production that does not rely on new, or distantly produced, nutrients; Dugdale and Goering, 1967). Bacteria also play a crucial role in the consumption of dissolved and particulate organic carbon (i.e., bacterial production, BP, Figure 1a; e.g., Garneau et al., 2008), which can then be transferred to higher trophic levels *via* the microbial loop (as described first by Azam et al., 1983). Bacterial production is coupled with bacterial respiration (BR), which produces dissolved inorganic carbon, i.e., CO_2, and may, therefore, represent a CO_2 source for the atmosphere (e.g., Nguyen et al., 2012). Bacterial respiration can represent the majority of the community respiration in the ocean (Robinson, 2008) and is, therefore, an important component of the oceanic carbon budget.

Bacterial growth efficiency (BGE) describes the proportion of organic carbon utilized by bacteria (i.e., the bacterial carbon demand, BCD), which is channeled into new biomass (BP), the rest being respired

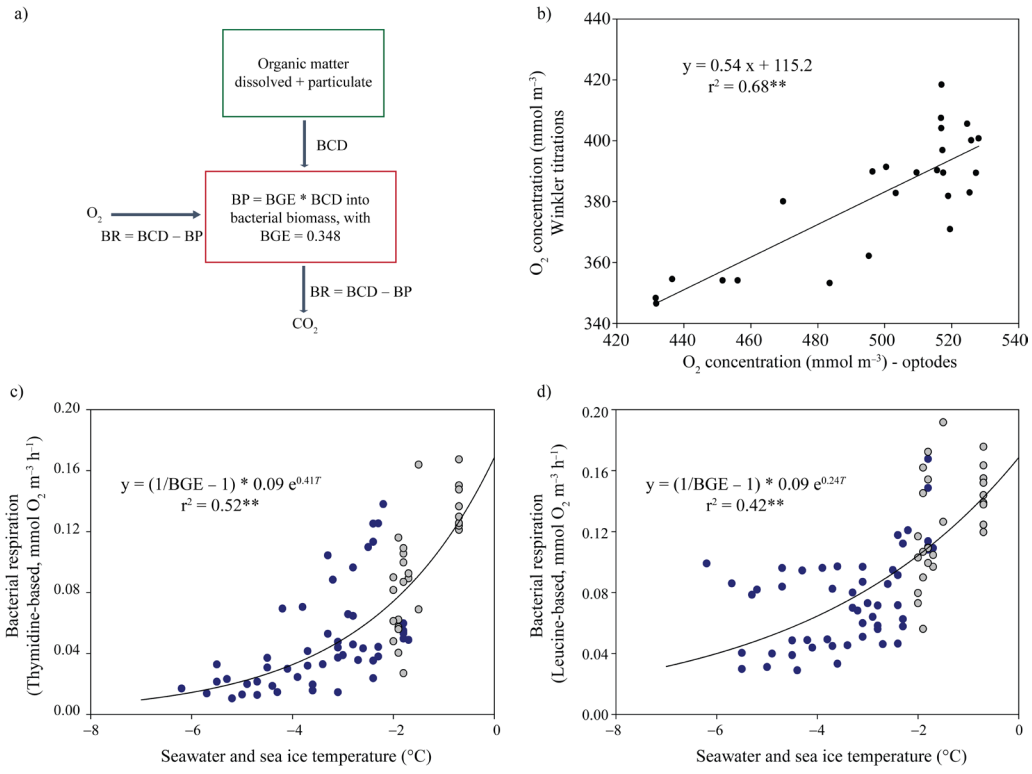

Figure 1

Schematic of bacterial production and respiration in the model, measured O_2 concentration and bacterial respiration.

a) Schematic of bacterial production and respiration in the model. Bacterial biomass is produced from dissolved and particulate organic carbon. Bacterial production (BP) corresponds to a given percentage (BGE: the bacterial growth efficiency) of the total bacterial carbon demand (BCD). The BCD that is not channelled into bacterial biomass is respired, giving the bacterial respiration: BR = BCD – BP. Processes and the associated rates are described in further detail in Materials and Methods. b) Linear regression between the O_2 concentrations (mmol m^{-3}) measured with Winkler titrations and optodes. Observed bacterial respiration rates (mmol O_2 m^{-3} h^{-1}) based on c) thymidine incorporation and d) leucine incorporation as a function of temperature (°C) and for BGE = 0.348. In Figure 1c and 1d, we included BR in seawater (grey circles) and in sea ice (blue circles) to extend the range of temperature and increase the confidence in the relationship between BR and *T*. For sea ice BR, we considered the data normalized to both salinity and to the starting conditions, following Zhou et al. (2014). An exponential regression line indicates the relationship between the two variables. Significance is indicated: * * for $p < 0.01$

doi: 10.12952/journal.elementa.000080.f001

and channeled into CO_2 (BR). The bacterial growth efficiency (BGE) in aquatic ecosystems ranges from < 0.05 to 0.6 (del Giorgio and Cole, 1998) and is typically higher at low temperatures where temperature-related respiratory losses are smaller. The mean estimate for BGE in seawater at below-zero (–2 to 0°C) temperatures that has been used previously is 0.348 (Kuparinen and Bjørnsen, 1992; Rivkin and Legendre, 2001; Nguyen and Maranger, 2011; Kaartokallio et al., 2013). However, bacterial respiration remains poorly constrained in sea ice and seawater from polar regions (Nguyen and Maranger, 2011), where BGEs range from 0.2 to 0.58 (Kuparinen and Bjørnsen, 1992; Rivkin and Legendre, 2001; Kuparinen et al., 2011; Nguyen and Maranger, 2011).

To date, estimates of bacterial production and respiration are limited in polar oceans and especially within and below sea ice, representing a fundamental gap in our knowledge of the biogeochemical cycle of carbon and of the fate of organic carbon in these oceans (Vancoppenolle et al., 2013). Bacterial respiration may represent 45%, on average, of the respiratory losses for the global ocean (Robinson, 2008) with a range of 25% to 90% for polar and sub-polar regions (Sherr and Sherr, 1996; Robinson et al., 1999; Rivkin and Legendre, 2001; Kirchman et al., 2005). Because of this broad range, there are still obviously large uncertainties on the quantitative role of bacterial respiration in polar oceans.

Net biological activity, i.e., the sum of oxygen production and respiration, can be determined from dissolved O_2 measurements. Thus, the determination of O_2 dynamics in and under the sea ice can lead to a better grasp on the role of biological activity in biogeochemical cycles in ice-covered ecosystems. This paper focuses on bacterial processes (i.e., BR and BP). However, we fully appreciate that, in the field, primary production is also a key factor determining O_2 dynamics (Long et al., 2012). In addition, in the vicinity of sea ice, or directly within sea ice, O_2 dynamics are influenced by physical sea ice processes (i.e., the incorporation/release of oxygen by sea ice growth/melt, brine drainage and flushing; Tsurikov, 1979) and by gas-specific processes such as the formation of gas bubbles due to gas supersaturation (Tison et al., 2002; Light et al., 2003) and direct ice-atmosphere gas fluxes (Delille, 2006; Nomura et al., 2010a).

The objective of this study was to assess the O_2 budget in the water under sea ice, combining observations (in an idealized experimental system) and modelling (a one-dimensional ice-ocean physical biogeochemical model). We used data from a controlled ice-growth experiment where the microbial community was composed solely of heterotrophic bacteria (primary producers and larger heterotrophic organisms were absent). Modelling was used to discriminate between physical processes (ice growth/melt, brine drainage, flushing), gas-specific transport (ice-atmosphere gas fluxes and gas bubble formation in sea ice) and bacterial respiration. In addition, the model was used to constrain BGE in cold under-ice water and, thus, to estimate the proportion of organic carbon utilized by bacteria, which is channeled into new biomass (particulate form) or respiration (CO_2).

Material and methods

Experimental and laboratory methods

This study presents part of the results from an ice-tank experiment (INTERICE V) at the Arctic Environmental Test Basin of the Hamburg Ship Model Basin (HSVA-Hamburg, Germany). Sea ice was grown in 1 m^3 mesocosms (filled with seawater from the North Sea) under controlled conditions during a 19-day experiment (for a detailed description of the experiment setup, see: Zhou et al., 2014; Jørgensen et al., 2015). In brief, the experiment consisted of a 14-day freezing period where the air temperature was maintained at −14 °C, followed by a 5-day warming period where the air temperature was increased to −1 °C. Throughout the experiment the water under the ice was fully mixed using a submersible pump. Here, we only report results from a treatment where North Sea water was used (SW in Zhou et al., 2014). This particular treatment had no obvious terrestrial humic components as described in Jørgensen et al. (2015) and DOC concentration averaged 140.7 ± 4.3 µmol L^{-1}. In addition, inorganic nutrients were added in excess (with initial concentrations of 26 ± 2 µmol N L^{-1} and 1.9 ± 0.1 µmol P L^{-1}) to avoid limiting bacteria. According to Zhou et al. (2014), nutrient concentrations did not show obvious changes during the course of the experiment. Unless explicitly mentioned, we only report results from the seawater underneath sea ice where continuous measurements of O_2 were performed, and not from the sea ice cover itself.

Salinity and temperature were measured with a Valeport miniCTD (Valeport, UK) operating in continuous mode at 1Hz throughout the experiment. The CTD probe was calibrated at the Finnish Meteorological Institute, Helsinki, Finland, as part of regular QA in-house CTD calibration. The CTD probe was placed in the seawater 50 cm under the sea ice. The O_2 concentration in the underlying seawater was measured continuously with PreSens OXY-4 Micro (PreSens, Germany) four-channel optodes at 1 minute intervals throughout the 19 day experiment. The oxygen microsensors with measuring tip diameter of 140 µm were placed at a depth approximately 50 cm under the growing sea ice. Any ice-crystal formation around the micro-sized sensor tips would have led to a clear discontinuity in oxygen concentration measurement (Mock et al., 2002). Because no such discontinuity was observed, we assumed that no crystal formation occurred around the sensor tips. In addition to the optode sensors, 50-ml water samples were taken every day for the measurement of dissolved oxygen using conventional Winkler titration methods. The O_2 concentrations measured with both techniques were significantly correlated ($r^2 = 0.68$, $p < 0.01$; Figure 1b). This relationship is not strong. However, because we operated the optode instrument below its nominal temperature range (ending at 0 °C) at a relatively high salinity, we considered Winkler titrations to be more reliable (Tengberg et al., 2006; Uchida et al., 2008). Because optode measurements were continuous, we used the optodes-Winkler correlation to calibrate the optode measurements. In the rest of the manuscript, we report those calibrated measurements.

The absence of primary producers and larger heterotrophic organisms was verified daily by epifluorescence microscopy. Bacterial production (BP in mmol O_2 m^{-3} h^{-1}) was measured using the ^{14}C-leucine (Leu) and ^{3}H-thymidine (TdR) incorporation methods simultaneously with dual labelling. Ice core sections were crushed using a spike and electrical ice cube crusher. A 10 ml sample of crushed ice was weighed in a scintillation vial with 2–4 ml of filtered (on 0.2 µm filters) seawater from the sample bags, in order to better simulate the salinity of the brine environment inside ice. The samples were incubated at −0.6°C on crushed ice and in the dark. The incubation time was 19–22 h for ice samples and 4–6 h for water and brine samples. To calculate BP from TdR incorporation, we used a carbon conversion factor of 75.2 kg C mol^{-1} (Nagata and Watanabe, 1990; Smith and Clement, 1990; Pelegrí et al., 1999; Kaartokallio, 2004). To calculate BP from Leu incorporation, we used a carbon conversion factor of 3 kg C mol^{-1} (Bjornsen and Kuparinen, 1991). Bacterial abundance was measured by flow cytometry using an LSRII (Becton Dickinson, USA) flow cytometer and SYBR Green II dye. Total bacterial abundance and abundance of low/high nucleic acid containing (LNA/HNA) bacteria were determined from bivariate plots of right-angle light scatter and green fluorescence.

We considered that BP (the net bacterial production) corresponds to a given percentage (BGE: the bacterial growth efficiency) of the total bacterial carbon demand (BCD, i.e., the gross bacterial production; see Figure 1a for a schematic of bacterial production and respiration). In this study, we first considered a BGE value of 0.348, which is an average value of those reported by Kuparinen and Bjørnsen (1992); Rivkin and Legendre (2001), and which is commonly used for polar oceans studies (Nguyen and Maranger, 2011). Accordingly, we first calculated the bacterial carbon demand by considering that BP = BGE * BCD. Then, we calculated bacterial respiration as:

$$BR = BCD - BP = (1 / BGE - 1) * BP \quad (1)$$

BR in carbon units was then converted to O_2 units assuming a respiratory quotient of 1 (Kaartokallio et al., 2013) which falls in the range of 0.8 to 1.2 for respiratory quotients reported in marine systems (Oviatt et al., 1986; Robinson et al., 2002). Finally, to best estimate the role of BR in O_2 dynamics in the present study, we used a sensitivity analysis to optimize BGE (see below).

The model

To mimic the conditions observed during the INTERICE V experiment, we used the one-dimensional halo-thermodynamic sea ice model (LIM1D) of Vancoppenolle et al. (2010) which includes sea ice gas dynamics (i.e., the formation of gas bubbles in sea ice and ice-atmosphere gas fluxes, Moreau et al., 2014, 2015). Briefly, during ice formation, the concentration of impurities (including gases) increases in brine inclusions and leads to the increase in the partial pressure of gases, which theoretically leads to the formation of bubbles as those observed in sea ice by Tison et al. (2002) and Light et al. (2003). Moreover, indirect evidence (Zhou et al., 2013; Moreau et al., 2014) shows that, because of their buoyancy, gas bubbles rise through the brine network, given that the brine volume is large enough to allow passage. During the present experiment, the brine volume was always above 7% (Zhou et al., 2014) allowing the rise and escape of gas bubbles (Zhou et al., 2013), as well as ice-atmosphere gas exchanges (Golden et al., 1998), as observed for CO_2 (Kotovitch et al., 2015). Once gas bubbles reach the surface of the ice, they escape and add to the diffusive part of ice-atmosphere O_2 fluxes. The simulation spans days 1 to 19 of the experiment, and the model reproduced well sea ice growth and melt during the experiment, i.e., the difference between the modelled and observed ice thickness averaged 1.19 ± 0.16 cm (Figure 2a).

Seawater model component

We added a dynamic seawater module to LIM1D. To do so, at each time step, we first calculated the change in water level in the tank (h_w, in m), due to ice growth or melt ($\partial h_i/\partial t$, in m h^{-1}, positive for an increase in ice thickness), assuming that the total mass of H_2O is conserved:

$$\partial h_w / \partial t = - \rho_{ice} / \rho_{water} * \partial h_i / \partial t \quad (2)$$

where ρ_i and ρ_w are the sea ice and seawater densities, respectively (in kg m^{-3}).

To update the concentration of the n^{th} tracer in seawater C^n_w (in mmol m^{-3}), we assumed that any change in the mass of tracer is due to an input from the ice above:

$$\partial(C^n_w h_w) / \partial t = F^n \quad (3)$$

where F^n is the tracer flux (in mmol m^{-2} h^{-1}, positive to the seawater), including sea ice growth and melt and brine drainage contributions (see Vancoppenolle et al., 2010). After the change in the mass of tracer in the seawater due to ice-ocean fluxes has been calculated, the change in the mass of tracer due to bacterial respiration is calculated (see below).

The above assumption is, however, not strictly valid and there was another potential source/sink of O_2 for the seawater below sea ice. To avoid pressure build-up within the tank, a 7-cm diameter and 70-cm deep tube was placed on the side of each mesocosm. The tubes were cleared of ice every day, during the entire experiment. Potential in/out air-water fluxes should therefore be taken into account in our gas tracer budgets. However, incremental computations of the air-seawater O_2 transfer, made using the seawater O_2 concentration, the gas transfer velocity over a small lake at a low wind speed (Crusius and Wanninkhof, 2003) and the Schmidt number taken from Wanninkhof (1992), show that the daily impact of pressure pipes on the O_2 concentration of the underlying water equalled ~ 0.01%: the potential O_2 exchange was 0.035 mmol of O_2 d^{-1}, compared to a total seawater O_2 quantity of ~ 340 mmol m^{-3}. In fact, this value is an overestimation since rapid refreezing of water within the tube hampered O_2 exchange most of the time. We assume, therefore, that it was negligible.

Bacterial respiration model component

Temperature is a major controlling factor of bacterial respiration, particularly in polar and temperate regions (Robador et al., 2009; Sarmento et al., 2010). This concept was supported further by the present experiment where temperature appeared to be the major controlling factor for BR in sea ice and seawater. BR and T were strongly correlated, particularly when the relationship was determined between T and TdR-based BR estimates ($r^2 = 0.52$, $p < 0.01$; Figure 1c). The correlation between T and Leu-based BR estimates was not as strong although it was significant ($r^2 = 0.42$, $p < 0.01$; Figure 1d).

On the contrary, during the INTERICE V experiment, TdR-based and Leu-based BR estimates were not significantly related to total bacterial abundance or the abundance of HNA and LNA bacteria (Table 1). Although BR followed the dynamics of sea ice and seawater temperature (Zhou et al., 2014), bacterial abundance did not, particularly during ice melt. During ice growth, both BR and bacterial abundance were highest near the bottom of sea ice, where temperature was the highest. However, during ice melt, when the ice was warm, bacterial abundance dropped, presumably because of brine dilution, while BR was high throughout the whole ice column.

Table 1. Correlations between bacterial respiration and temperature, total bacterial abundance, high nucleic acid bacteria, low nucleic acid bacteria and dissolved organic carbon (DOC)[a]

r - values	T[e]	TB[f]	HNA[g]	LNA[h]	DOC[i]
BR[b] - TdR-based[c]	0.52**	0.002	0.004	0.005	0.29**
BR[b] - Leu-based[d]	0.42**	0.08	0.09	0.001	0.4**

[a]Relationships between variables were tested with model II linear regression analyses. R^2 values and significance are indicated: ** for $p < 0.01$.
[b]Bacterial respiration (mmol O_2 m^{-3} h^{-1}) measured in both sea ice and seawater
[c]BR estimates based on the thymidine incorporation method
[d]BR estimates based on the leucine incorporation method
[e]Temperature (°C) in both sea ice and seawater
[f]Total bacterial abundance (cells ml^{-1})
[g]High nucleic acid bacteria (cells ml^{-1})
[h]Low nucleic acid bacteria (cells ml^{-1})
[i]Dissolved organic carbon (µmol l^{-1})
doi: 10.12952/journal.elementa.000080.t001

In addition, BR correlated negatively with the concentration of dissolved organic carbon (DOC, $r^2 = 0.29$, $p < 0.01$ for TdR-based BR estimates; $r^2 = 0.4$, $p < 0.01$ for Leu-based BR estimates). However, bacterial respiration showed the strongest relationship with, and was best determined by, temperature. Hence, in the model, we parameterize BR in seawater and sea ice (in mmol O_2 m^{-3} h^{-1}) based on the strong T-BR relationship observed in both seawater and sea ice (Figure 1c and 1d). We used an exponential type of regression to relate BR and T:

$$BR = \alpha * e(r_g * T) \quad (4)$$

where r_g is the temperature-dependent rate of growth and α is a fixed coefficient which is equivalent to $BR|^{0°C}$. Therefore, in the model, BR, and the oxygen uptake per unit time associated with bacterial respiration (mmol O_2 m^{-3} h^{-1}), can be determined from temperature as:

$$BR = \partial O_2 / \partial t \,|_{BR} = BR\,|^{0°C} * e^{(r_g * T)} = (1 / BGE - 1) * BP\,|^{0°C} * e^{(r_g * T)} \quad (5)$$

To determine r_g and BP at 0 °C (denoted as $BP|^{0°C}$), we used a two-parameter regression analysis. For TdR-based BR estimates, we have $r_g = 0.41$ and $BP|^{0°C} = 0.09$ mmol O_2 m^{-3} h^{-1} (Pearson correlation coefficient, $r^2 = 0.52$, $p < 0.01$). For Leu-based BR estimates, we obtain $r_g = 0.24$ and $BP|^{0°C} = 0.09$ mmol O_2 m^{-3} h^{-1} ($r^2 = 0.42$, $p < 0.01$).

The advantage of this approach is that BGE can be fitted without modifying $BP|^{0°C}$. For the sensitivity analysis presented below, where we fit BGE to best estimate the role of BR in O_2 dynamics, we used BGE values of 0.348, 0.4, 0.45 and 0.5. In the present study, we have more confidence in the TdR-based respiration estimates. This confidence is based on the more robust relationship between TdR-based respiration estimates and temperature (r^2 value of 0.52) than the relationship between Leu-based respiration estimates and temperature (r^2 value of 0.42).

Finally, based on the present observations, the model was run with initial seawater and sea ice O_2 concentration of 340 mmol m^{-3} and 68 mmol m^{-3}, respectively. The conservation of the total sea ice and seawater O_2 content minus the ice-atmosphere O_2 fluxes (negative to the ice) was checked at the end of each model time step. Ten vertical ice layers discretized the vertical dimension; the time step was 1h.

Results and discussion

Salinity

Seawater salinity changed according to salt fluxes between sea ice and the water underneath. The model reproduces the observations with good accuracy in sea ice (where the difference in bulk ice salinity between the model and the observations averaged 1.27 ± 0.34 g kg^{-1}, Figure 2a) and in the seawater (where the difference in seawater salinity between the model and the observations averaged 0.38 ± 0.006 g kg^{-1}). The observed and simulated salinity of the under-ice water increased during ice growth (from day 0 to 14) due to brine rejection and drainage (Figure 2b). During ice melt (from day 15 to 20), the observed and simulated salinity of the under-ice water decreased due to freshwater release from the melting ice. Dilution effects during the melting phase are, however, somewhat underestimated by the model. In the text below, we refer to these latter processes as physical processes: i.e., fluxes of sea ice-ocean tracers due to ice growth and melt (including basal growth or melt and surface melt), brine convection and diffusion as described in Vancoppenolle et al. (2010).

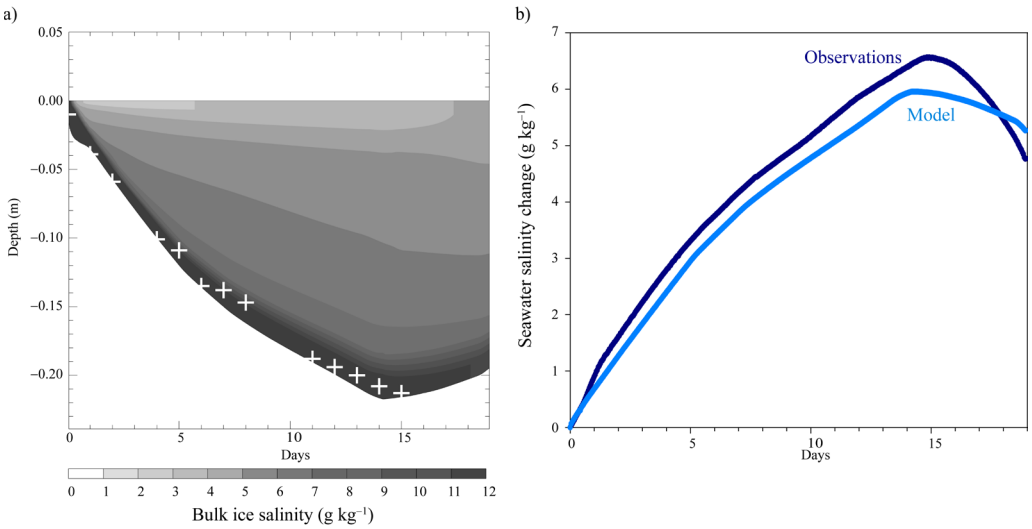

Figure 2

Simulated bulk ice salinity and changes in observed and simulated seawater salinity.

a) Simulated bulk ice salinity (g kg^{-1}) along with observed ice thickness (white crosses). b) Changes in observed (i.e., CTD probe, dark blue line) and simulated (light blue line) seawater salinity (g kg^{-1}). In Figure 2a, it should be noted that, during ice growth, salinity increases near the surface of the ice artificially due to the increase in the thickness of the 10 ice layers at the end of each time step. For the particular case of the surface ice layer (1st layer), this increase in thickness results in an increase in salt content because this layer captures some of the salt content of the underlying (2nd) layer. This phenomenon is an artefact of the model, but given how small it is (< 2 g kg^{-1}), it can be ignored without modifying the conclusions of the output.

doi: 10.12952/journal.elementa.000080.f002

Drivers of O_2 concentration in seawater

As described by Mock et al. (2002) for a similar experimental study, we observed an increase in the O_2 concentration in the seawater below sea ice, followed by a decrease (brown curve in Figure 3a). This pattern is consistent with observations that growing sea ice releases brine enriched in O_2 while melting ice is undersaturated in O_2 (Glud et al., 2002). To understand the factors that drove O_2 dynamics in the water under sea ice during the present experiment, we first ran the model with no BR (in sea ice or seawater) and no gas specific transport (i.e., ice-atmosphere gas fluxes and gas bubbles buoyancy). In this run (the black curve in Figure 3a), the model reproduces the increase in O_2 concentration in the seawater below sea ice, followed by a decrease, but increasingly overestimates the O_2 concentration within the seawater.

We included ice-atmosphere gas fluxes and the formation of gas bubbles in sea ice in a second run (the "no respiration" run, dark blue curve in Figure 3a) to estimate their role in O_2 dynamics in the water under sea ice. In this run, the model also reproduces the increase in O_2 concentration in the seawater below sea ice, followed by a decrease, but still overestimates the O_2 concentration within the seawater. A large part of the seawater O_2 is, therefore, released to the atmosphere through ice-atmosphere gas fluxes and the formation of gas bubbles. However, this loss of O_2 is not large enough to completely explain the observed O_2 dynamics within the seawater in the present experiment.

In order to fully represent the O_2 concentration within the seawater, we included both gas-specific transport as well as BR in sea ice and in seawater as a function of temperature. When included, BR in both seawater and sea ice consume O_2 and give a better representation of O_2 within the seawater (Figure 3a). Thus, our modelling approach indicated that, in the closed system experimental conditions encountered at INTERICE V, gas-specific transport and, most importantly, BR play a significant role in the dynamics of O_2 underneath growing sea ice. At the end of the ice-growth period (day 14) gas-specific transport and BR (based on TdR estimates and a BGE of 0.4) had reduced the increase in the O_2 concentration by 37%, BR being responsible for 76% of this decrease.

We are somewhat confident in this result given the previous evaluation of the model, which rather well simulated the observed (e.g., Nomura et al., 2010a, 2010b; Miller et al., 2011; Papakyriakou and Miller, 2011; Geilfus et al., 2013; Nomura et al., 2013; Delille et al., 2014) amplitude and seasonality of ice-atmosphere gas fluxes and gas bubble formation rates (Moreau et al., 2014, 2015). It should, however, be considered that there are still uncertainties for this model, which does not capture all processes related to sea ice-atmosphere gas fluxes (e.g., wind pumping). In addition, the sea ice conditions reported here for the INTERICE V experiment, during which sea ice was permeable to gas fluxes, may not always apply to the field, in particular during the cold Arctic winter. For example, Zhou et al. (2013) reported very cold sea ice (with a brine volume < 5%) in winter 2009 from Barrow Point, Alaska. However, winter sea ice is not always impermeable to gas exchanges, especially when a thick snow layer covers it as was observed in winter by Sievers et al. (2015) at their DNB site in Young Sound, northeast Greenland. In addition, Nomura et al. (2006) reported CO_2 fluxes between sea ice and the atmosphere of −3.6 to +1 mmol m^{-2} d^{-1} for a cold landfast sea ice in February–March in Hokkaido Bay, Japan. During this latter study, the brine volume of sea ice was above the threshold of 5% (Golden et al., 1998) even though sea ice was sampled in winter during the growth phase. Therefore, the INTERICE V experiment is representative of these latter field studies during which sea ice was permeable to gas fluxes.

It should also be noted that BR in sea ice only plays a limited role in O_2 dynamics in the water under sea ice compared to BR in seawater. To determine the role of BR in sea ice, we ran the model with only BR in

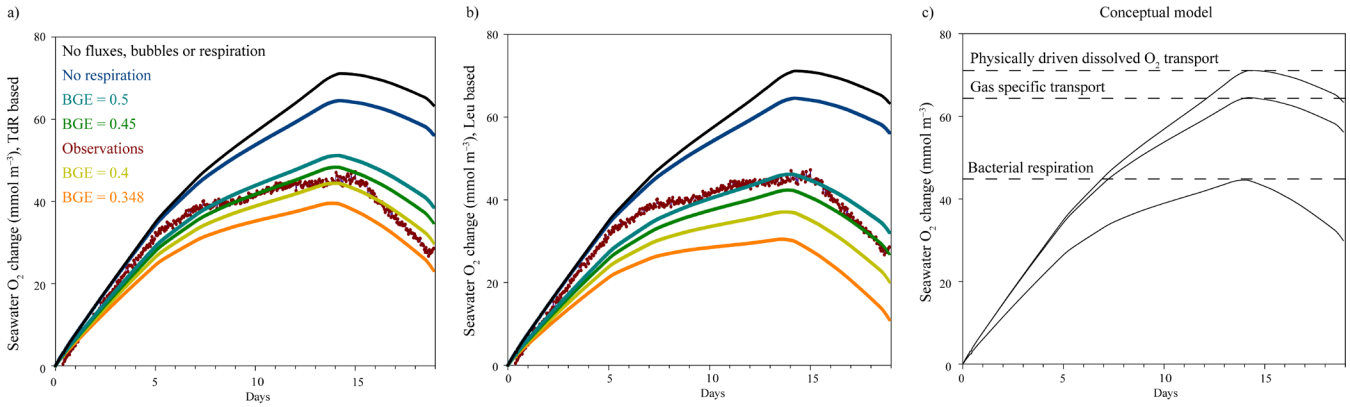

sea ice (i.e., with no ice-atmosphere gas fluxes, no bubbles in sea ice and no BR in seawater). The results of this run were similar to the "no fluxes, bubbles or respiration" run (i.e., the black curve in Figure 3a). In fact, the difference in the change in O_2 concentration between the two runs was less than 0.7%. This result implies that BR in sea ice may have an effect on O_2 within sea ice itself but has almost no impact on the change in O_2 concentration in the seawater below sea ice. This difference may have been due to the lower temperature as well as the lower bacterial abundance in sea ice (0.1 to 0.8 10^6 cells ml^{-1}) than in the seawater (0.9 to 1.0 10^6 cells ml^{-1}) and the lower cell-specific BP in sea ice compared to seawater (Zhou et al., 2014). In addition, the impact of sea ice BR is mostly on O_2 dynamics within sea ice, with the signal decreasing for the seawater below sea ice or the atmosphere above.

Fitting of the bacterial growth efficiency (BGE)

We, then, fitted BGE to best estimate the role of BR in O_2 dynamics in the seawater. First, we used TdR-based respiration estimates. When a BGE of 0.348 is used in the model (orange curve in Figure 3a), respiration is too high, i.e., it consumes too much O_2, and O_2 in the seawater is underestimated. With a BGE between 0.4 and 0.45, however, respiration consumes O_2 at an appropriate rate, and the model gives an accurate representation of the O_2 measurements made (yellow and green curves in Figure 3a). Finally, with a BGE of 0.5, respiration is too low and leads to an overestimation of O_2 in the under-ice seawater. We also fitted the BGE by using Leu-based respiration estimates. This analysis showed that BR is over-estimated when using a BGE of 0.348 and 0.4 (Figure 3b). A BGE value between 0.45 and 0.5, however, gives an accurate representation of O_2 observations in seawater when using Leu-based BR estimates. Therefore, the respiration estimates based on both thymidine and leucine bring similar results concerning the fitting of the BGE. Thus, we are confident that, during the present experiment, BGE was between 0.4 and 0.5 and BP in the under-ice seawater represented between 40% and 50% of BCD, the rest being BR.

A BGE between 0.4 and 0.5 as suggested by our sensitivity estimates can be considered realistic as BGEs in aquatic ecosystems range from < 0.05 to 0.6, depending on the quality of the dissolved organic matter that is used by bacteria (del Giorgio and Cole, 1998). Kuparinen et al. (2011) observed BGEs up to 0.58 in Baltic Sea ice. In addition, Rivkin and Legendre (2001) did a literature review of BGE values and found that BGE increased with lowering temperature (Figure 1 in Rivkin and Legendre, 2001). Their linear regression between BGE and temperature gives a BGE between 0.4 and 0.5 at 0°C, which is consistent with our estimates. However, other uncertainties still exist in the factors used to convert thymidine and leucine incorporation rates to BP and BR (e.g., Ducklow et al., 2000), in the respiratory quotients used (Oviatt et al., 1986; Robinson et al., 2002) or in the parameterization of ice-atmosphere gas fluxes in the model.

This fitted BGE of 0.4 to 0.5 also suggests that growth conditions were favourable for bacteria in seawater underneath sea ice during the experiment, which may be due to the rejection of bioavailable dissolved organic matter (DOM) from sea ice. During the present experiment, Jørgensen et al. (2015) measured the bioavailability of DOC at 16 ± 12% in the seawater below sea ice and as high as 45% in sea ice brines. The authors attributed this high bioavailability of DOC to abiotic processes related to sea ice formation. This explanation also suggests that bacteria underneath sea ice play an important role in polar oceans and may consume an important part of the organic carbon produced in sea ice as observed by Nguyen and Maranger (2011) in the Amundsen Gulf. It should, however, be remembered that primary producers were not present in this experiment.

Due to the low water temperature, the BR rates simulated in the tank were moderate (average of 7.9 ± 3.1 × 10^{-2} mmol O_2 m^{-3} h^{-1} for a BGE of 0.4). These BR rates are comparable to those measured by Kaartokallio et al. (2013) in sub-arctic sea ice, which ranged from 2.2 to 14 × 10^{-2} mmol O_2 m^{-2} h^{-1}

Figure 3

Observed and modelled changes in the seawater O_2 concentration.

Observed and modelled changes in the seawater O_2 concentration (mmol m^{-3}) with the modelled bacterial respiration based on a) thymidine incorporation and b) leucine incorporation (see Materials and methods for a description of how BR is retrieved from temperature in the model). The brown points indicate observed O_2 concentrations. The results of the different simulations are plotted as: BGE = 0.348 (orange curve), BGE = 0.4 (yellow curve), BGE = 0.45 (green curve), BGE = 0.5 (light blue curve), "no respiration" (dark blue curve) and "no fluxes, bubbles or respiration" (black curve). c) Conceptual model of the main biogeochemical processes that drove O_2 dynamics in the water under sea ice in the present experiment. The "Physically driven dissolved O_2 transport" curve corresponds to the sole effect of ice-ocean O_2 fluxes that mimic ice-ocean salt fluxes. The "gas specific transport" curve corresponds to the additive effect of ice-atmosphere fluxes and gas bubbles on O_2 concentration in the water under sea ice. Finally, the "bacterial respiration" curve corresponds to the additive effect of BR on O_2 in the water under sea ice. This curve was constructed from TdR-based respiration estimates and a BGE of 0.4.

doi: 10.12952/journal.elementa.000080.f003

(hence, from ~ 3×10^{-2} to 23 10^{-2} mmol O_2 m^{-3} h^{-1} given an average ice depth of ~ 60 cm), and to those measured by Nguyen et al. (2012) in seawater in the Amundsen Gulf which ranged from 1.3 to 12.6×10^{-2} mmol O_2 m^{-3} h^{-1}. However, even the moderate respiration rates reported here have a large impact on the O_2 budget in the water under the ice.

Conceptual model of O_2 dynamics in seawater under sea ice

Our data strongly suggest that, through the growth and decay cycle of the experimental sea ice we studied (i.e., where primary producers were absent), O_2 dynamics are controlled by physical processes (brine rejection or dilution by meltwater), gas specific transport (i.e., ice-atmosphere gas fluxes and gas bubble buoyancy) and BR. During ice growth, gas specific transport and BR (using a TdR-based estimates and a BGE of 0.4) reduced by ~37% the increase in O_2 concentration in seawater compared to a run without gas specific transport and BR (the so-called "physically driven dissolved O_2 transport" run in Figure 3c). In addition, during ice melt, gas specific transport and BR decreased the O_2 concentration in seawater by an additional 48% (Figure 3c).

Glud et al. (2014) suggested that during ice melt in the Fram Strait, O_2 exchange at the ice-water interface is dominated by physical (ice melt) rather than biological processes. In contrast, Long et al. (2012) deduced that biological activity controlled much (87%) of the observed O_2 fluxes between sea ice and seawater during ice melt. Therefore, our estimates that gas-specific transport and BR during ice melt are responsible for a 37% lower O_2 concentration in seawater fall between these two scenarios. We believe that the differences between our results and these two studies come from the different sea ice melting rates observed in this study (~ 0.4 cm d^{-1} ≈ 4 L m^{-2} d^{-1}), compared to 25 L m^{-2} d^{-1} in the study of Glud et al. (2014) and 0.8 mm d^{-1} (≈ 0.8 L m^{-2} d^{-1}) in the study of Long et al. (2012).

In addition, Long et al. (2012) and Glud et al. (2014) both observed a natural system where bacterial respiration occurred along with primary production, which was not the case in the present experiment. In these two studies, however, the seawater under sea ice was net heterotrophic with a consumption of O_2 of 1.45 mmol m^{-2} day^{-1} (Long et al., 2012) and 0.32 mmol m^{-2} day^{-1} (Glud et al., 2014). Moreover, the authors did not consider the potential effect of ice-atmosphere O_2 fluxes, while the formation of gas bubbles was unlikely in the systems they studied as sea ice was melting and depleted in O_2 in both cases. Indeed, gas bubbles usually form during ice growth when gases are concentrated within brines (Moreau et al., 2014).

It should also be noted that the very shallow depth (1 m) of the tanks used in the present study strongly amplified the importance of physical processes over respiration and gas-specific transport compared to *in situ* studies where the mixed layer depth is significantly deeper. For instance, Toole et al. (2010) measured average mixed layer depths of 16 m and 24 m during, respectively, summer and winter in the Canada Basin. Barthélemy et al. (2015) reported mixed layer depths between 25 m and 35 m in the Arctic basin from the MIMOC climatology (Monthly Isopycnal and Mixed layer Ocean Climatology). During ice melt, on the contrary, the shallow depth of the tanks used in the present experiment may well represent the depth (e.g., 0.5 m) of the thin meltwater layer that is sometimes observed underneath melting sea ice (e.g., Assmy et al., 2013). Therefore, our results emphasize that BR and gas specific transport may dominate under-ice water O_2 fluxes depending on the depth of the upper mixed layer.

Conclusions

In the present paper, the O_2 budget in an idealized experimental system with no primary producers could be assessed, with the help of a one-dimensional ice ocean physical biogeochemical model. Our confidence in the physical ability of the model is high given the faithful representation of salinity in the water under ice and reinforced by the fact that the changes in oxygen in water are also well represented.

We argue that bacterial respiration was the dominant biogeochemical driver of O_2 concentrations in the water under ice, followed by gas specific transport (i.e., ice-atmosphere O_2 fluxes, gas bubble formation and rise). The model suggests that the actual contribution of BR and gas specific transport to the change in seawater oxygen concentration was 37% during ice growth and 48% during melt. The magnitude of that impact will, however, critically depend on the mixed layer depth *in situ*.

The bacterial growth efficiency in the water under sea ice, as retrieved from a simulated O_2 budget, was found to be between 0.4 and 0.5, which is in line with the published BGE values for cold seawater. Furthermore, this relatively high BGE suggests that growth conditions under the ice were favourable for bacteria. It should, however, be considered that our estimation of BGE would change in a natural polar system where labile DOM is produced and released by phytoplankton and zooplankton grazing.

Given the important role of BR on O_2 in the present study, one may assume that bacterial respiration in and underneath sea ice plays an important role in polar oceans in terms of gas fluxes and, potentially, in terms of organic matter consumption as suggested by Nguyen and Maranger (2011).

Finally, we conclude that the parameterization developed here to describe the role of BR in determining O_2 in the water under sea ice is generally applicable in the context of large-scale ocean modelling applications. At the very least, the salient features identified here, namely the strong temperature dependence of

bacterial respiration and the high growth efficiency, should form, according to the experiment described in this paper, the basic characteristics of any representation of polar marine bacterial processes in biogeochemical ocean modelling applications, such as regional or large-scale Earth System models. This study illustrates that simple experiments and models ideally blend together for basic process understanding and quantification.

References

Assmy P, Ehn JK, Fernández-Méndez M, Hop H, Katlein C, et al. 2013. Floating ice-algal aggregates below melting Arctic sea ice. *PLoS ONE* **8**(10): e76599. doi: 10.1371/journal.pone.0076599.

Azam F, Fenchel T, Field JG, Gray JS, Meyer-Reil LA, et al. 1983. The ecological role of water-column microbes in the sea. *Mar Ecol-Prog Ser* **10**: 257–263.

Barthélemy A, Fichefet T, Goosse H, Madec G. 2015. Modeling the interplay between sea ice formation and the oceanic mixed layer: Limitations of simple brine rejection parameterizations. *Ocean Model* **86**: 141–152. doi: 10.1016/j.ocemod.2014.12.009.

Bjornsen PK, Kuparinen J. 1991. Determination of bacterioplankton biomass, net production and growth efficiency in the Southern Ocean. *Mar Ecol-Prog Ser* **71**: 185–194.

Crusius J, Wanninkhof R. 2003. Gas transfer velocities measured at low wind speed over a lake. *Limnol Oceanogr* **48**(3): 1010–1017.

del Giorgio PA, Cole JJ. 1998. Bacterial growth efficiency in natural aquatic systems. *Annu Rev Ecol Syst* **29**: 503–541.

Delille B. 2006. Inorganic carbon dynamics and air-ice-sea CO_2 fluxes in the open and coastal waters of the Southern Ocean. [Ph.D. Thesis]. Liège, Belgium: Université de Liège.

Delille B, Vancoppenolle M, Geilfus N-X, Tilbrook B, Lannuzel D, et al. 2014. Southern Ocean CO_2 sink: The contribution of the sea ice. *J Geophys Res-Oceans* **119**(9): 6340–6355. doi: 10.1002/2014JC009941.

Ducklow HW, Dickson M-L, Kirchman DL, Steward G, Orchardo J, et al. 2000. Constraining bacterial production, conversion efficiency and respiration in the Ross Sea, Antarctica, January-February, 1997. *Deep-Sea Res Pt II* **47**(15–16): 3227–3247.

Dugdale RC, Goering JJ. 1967. Uptake of new and regenerated forms of nitrogen in primary productivity. *Limnol Oceanogr* **12**: 196–206.

Fripiat F, Tison J-L, André L, Notz D, Delille B. 2014. Biogenic silica recycling in sea ice inferred from Si-isotopes: Constraints from Arctic winter first-year sea ice. *Biogeochemistry* **119**(1–3): 25–33. doi: 10.1007/s10533-013-9911-8.

Garneau M-È, Roy S, Lovejoy C, Gratton Y, Vincent WF. 2008. Seasonal dynamics of bacterial biomass and production in a coastal arctic ecosystem: Franklin Bay, western Canadian Arctic. *J Geophys Res-Oceans* **113**(C7): C07S91. doi: 10.1029/2007JC004281.

Geilfus N-X, Carnat G, Dieckmann GS, Halden N, Nehrke G, et al. 2013. First estimates of the contribution of $CaCO_3$ precipitation to the release of CO_2 to the atmosphere during young sea ice growth. *J Geophys Res-Oceans* **118**(1): 244–255.

Glud RN, Rysgaard S, Kühl M. 2002. A laboratory study on O_2 dynamics and photosynthesis in ice algal communities: Quantification by microsensors, O_2 exchange rates, ^{14}C incubations and a PAM fluorometer. *Aquat Microb Ecol* **27**(3): 301–311.

Glud RN, Rysgaard S, Turner G, McGinnis DF, Leakey RJG. 2014. Biological- and physical-induced oxygen dynamics in melting sea ice of the Fram Strait. *Limnol Oceanogr* **59**(4): 1097–1111.

Golden KM, Ackley SF, Lytle VI. 1998. The percolation phase transition in sea ice. *Science* **282**(5397): 2238–2241. doi: 10.1126/science.282.5397.2238.

Jørgensen L, Stedmon CA, Kaartokallio H, Middelboe M, Thomas DN. 2015. Changes in the composition and bioavailability of dissolved organic matter during sea ice formation. *Limnol Oceanogr* **60**(3): 817–830. doi: 10.1002/lno.10058.

Kaartokallio H. 2004. Food web components, and physical and chemical properties of Baltic Sea ice. *Mar Ecol-Prog Ser* **273**: 49–63. doi: 10.3354/meps273049.

Kaartokallio H, Søgaard DH, Norman L, Rysgaard S, Tison J-L, et al. 2013. Short-term variability in bacterial abundance, cell properties, and incorporation of leucine and thymidine in subarctic sea ice. *Aquat Microb Ecol* **71**(1): 57–73.

Kirchman DL, Malmstrom RR, Cottrell MT. 2005. Control of bacterial growth by temperature and organic matter in the Western Arctic. *Deep-Sea Res Pt II* **52**(24–26): 3386–3395. doi: 10.1016/j.dsr2.2005.09.005.

Kotovitch M, Moreau S, Zhou J, Vancoppenolle M, Dieckmann GS, et al. 2015. Measurements of air-ice CO_2 fluxes over experimental sea ice: A gas bubble transport hypothesis. *Elem Sci Anth*: Under review for this Special Feature.

Kuparinen J, Autio R, Kaartokallio H. 2011. Sea ice bacterial growth rate, growth efficiency and preference for inorganic nitrogen sources in the Baltic Sea. *Polar Biol* **34**(9): 1361–1373. doi: 10.1007/s00300-011-0989-y.

Kuparinen J, Bjørnsen PK. 1992. Spatial distribution of bacterioplankton production across the Weddell-Scotia Confluence during early austral summer 1988–1989. *Polar Biol* **12**(2): 197–204.

Light B, Maykut GA, Grenfell TC. 2003. Effects of temperature on the microstructure of first-year Arctic sea ice. *J Geophys Res-Oceans* **108**(2): 3051. doi: 10.1029/2001JC000887.

Long MH, Koopmans D, Berg P, Rysgaard S, Glud RN, et al. 2012. Oxygen exchange and ice melt measured at the ice-water interface by eddy correlation. *Biogeosciences* **9**(6): 1957–1967.

Miller LA, Papakyriakou TN, Collins RE, Deming JW, Ehn JK, et al. 2011. Carbon dynamics in sea ice: A winter flux time series. *J Geophys Res-Oceans* **116**(2): C02028. doi: 10.1029/2009jc006058.

Mock T, Dieckmann GS, Haas C, Krell A, Tison J-L, et al. 2002. Micro-optodes in sea ice: A new approach to investigate oxygen dynamics during sea ice formation. *Aquat Microb Ecol* **29**(3): 297–306.

Moreau S, Vancoppenolle M, Delille B, Tison J-L, Zhou J, et al. 2015. Drivers of inorganic carbon dynamics in first-year sea ice: A model study. *J Geophys Res-Oceans* **120**(1): 471–495.

Moreau S, Vancoppenolle M, Zhou J, Tison J-L, Delille B, et al. 2014. Modeling Argon dynamics in first-year sea ice. *Ocean Model* **73**: 1–18.

Nagata T, Watanabe Y. 1990. Carbon- and nitrogen-to-volume ratios of bacterioplankton grown under different nutritional conditions. *Appl Environ Microbiol* **56**(5): 1303–1309.

Nguyen D, Maranger R. 2011. Respiration and bacterial carbon dynamics in Arctic sea ice. *Polar Biol* **34**(12): 1843–1855. doi: 10.1007/s00300-011-1040-z.

Nguyen D, Maranger R, Tremblay J-É, Gosselin M. 2012. Respiration and bacterial carbon dynamics in the Amundsen Gulf, western Canadian Arctic. *J Geophys Res-Oceans* **117**(C9): C00G16. doi: 10.1029/2011JC007343.

Nomura D, Eicken H, Gradinger R, Shirasawa K. 2010a. Rapid physically driven inversion of the air-sea ice CO_2 flux in the seasonal landfast ice off Barrow, Alaska after onset of surface melt. *Cont Shelf Res* **30**(19): 1998–2004. doi: 10.1016/j.csr.2010.09.014.

Nomura D, Granskog MA, Assmy P, Simizu D, Hashida G. 2013. Arctic and Antarctic sea ice acts as a sink for atmospheric CO_2 during periods of snowmelt and surface flooding. *J Geophys Res-Oceans* **118**(12): 6511–6524.

Nomura D, Yoshikawa-Inoue H, Toyota T. 2006. The effect of sea-ice growth on air-sea CO_2 flux in a tank experiment. *Tellus, Ser B* **58**(5): 418–426. doi: 10.1111/j.1600-0889.2006.00204.x.

Nomura D, Yoshikawa-Inoue H, Toyota T, Shirasawa K. 2010b. Effects of snow, snowmelting and refreezing processes on air-sea-ice CO_2 flux. *J Glaciol* **56**(196): 262–270. doi: 10.3189/002214310791968548.

Oviatt CA, Rudnick DT, Keller AA, Sampou PA, Almquist GT. 1986. A comparison of system (O_2 and CO_2) and C-14 measurements of metabolism in estuarine mesocosms. *Mar Ecol-Prog Ser* **28**: 57–67.

Papakyriakou T, Miller L. 2011. Springtime CO_2 exchange over seasonal sea ice in the Canadian Arctic Archipelago. *Ann Glaciol* **52**(57): 215–224. doi: 10.3189/172756411795931534.

Pelegrí SP, Dolan J, Rassoulzadegan F. 1999. Use of high temperature catalytic oxidation (HTCO) to measure carbon content of microorganisms. *Aquat Microb Ecol* **16**(3): 273–280. doi: 10.3354/ame016273.

Rivkin RB, Legendre L. 2001. Biogenic carbon cycling in the upper ocean: Effects of microbial respiration. *Science* **291**(5512): 2398–2400.

Robador A, Brüchert V, Jørgensen BB. 2009. The impact of temperature change on the activity and community composition of sulfate-reducing bacteria in arctic versus temperate marine sediments. *Environ Microbiol* **11**(7): 1692–1703. doi: 10.1111/j.1462–2920.2009.01896.x.

Robinson C. 2008. Heterotrophic bacterial respiration, in Kirchman DL ed., *Microbial Ecology of the Oceans, 2 nd edition*. New York: John Wiley: pp. 299–327.

Robinson C, Archer SD, Williams PJLB. 1999. Microbial dynamics in coastal waters of East Antarctica: Plankton production and respiration. *Mar Ecol-Prog Ser* **180**: 23–36.

Robinson C, Serret P, Tilstone G, Teira E, Zubkov MV, et al. 2002. Plankton respiration in the Eastern Atlantic Ocean. *Deep-Sea Res Pt I* **49**: 787–813. doi: 10.1016/S0967-0637(01)00083-8.

Sarmento H, Montoya JM, Vázquez-Domínguez E, Vaqué D, Gasol JM. 2010. Warming effects on marine microbial food web processes: How far can we go when it comes to predictions? *Philos Trans R Soc B* **365**: 2137–2149. doi: 10.1098/rstb.2010.0045.

Sherr EB, Sherr BF. 1996. Temporal offset in oceanic production and respiration processes implied by seasonal changes in atmospheric oxygen: The role of heterotrophic microbes. *Aquat Microb Ecol* **11**: 91–100.

Sievers J, Sørensen LL, Papakyriakou T, Else B, Sejr MK, et al. 2015. Winter observations of CO_2 exchange between sea ice and the atmosphere in a coastal fjord environment. *The Cryosphere* **9**(4): 1701–1713. doi: 10.5194/tc-9-1701-2015.

Smith REH, Clement P. 1990. Heterotrophic activity and bacterial productivity in assemblages of microbes from sea ice in the high Arctic. *Polar Biol* **10**(5): 351–357.

Tengberg A, Hovdenes J, Andersson HJ, Brocandel O, Diaz R, et al. 2006. Evaluation of a lifetime-based optode to measure oxygen in aquatic systems. *Limnol Oceanogr: Methods* **4**(2): 7–17. doi: 10.4319/lom.2006.4.7.

Tison J-L, Haas C, Gowing MM, Sleewaegen S, Bernard A. 2002. Tank study of physico-chemical controls on gas content and composition during growth of young sea ice. *J Glaciol* **48**(161): 177–190.

Toole JM, Timmermans M-L, Perovich DK, Krishfield RA, Proshutinsky A, et al. 2010. Influences of the ocean surface mixed layer and thermohaline stratification on Arctic Sea ice in the central Canada Basin. *J Geophys Res-Oceans* **115**(C10): C10018. doi: 10.1029/2009JC005660.

Tsurikov VL. 1979. The formation and composition of the gas content of sea ice. *J Glaciol* **22**(86): 67–81.

Uchida H, Kawano T, Kaneko I, Fukasawa M. 2008. In situ calibration of optode-based oxygen sensors. *J Atmos Ocean Tech* **25**(12): 2271–2281. doi: 10.1175/2008JTECHO549.1.

Vancoppenolle M, Goosse H, De Montety A, Fichefet T, Tremblay B, et al. 2010. Modeling brine and nutrient dynamics in Antarctic sea ice: The case of dissolved silica. *J Geophys Res-Oceans* **115**(2). doi: 10.1029/2009jc005369.

Vancoppenolle M, Meiners K, Michel C, Bopp L, Brabant F, et al. 2013. Role of sea ice in global biogeochemical cycles: Emerging views and challenges. *Quat Sci Rev* **79**: 207–230.

Wanninkhof R. 1992. Relationship between wind speed and gas exchange over the ocean. *J Geophys Res-Oceans* **97**(C5): 7373–7382.

Zhou J, Delille B, Eicken H, Vancoppenolle M, Brabant F, et al. 2013. Physical and biogeochemical properties in landfast sea ice (Barrow, Alaska): Insights on brine and gas dynamics across seasons. *J Geophys Res-Oceans* **118**(6): 3172–3189. doi: 10.1002/jgrc.20232.

Zhou J, Delille B, Kaartokallio H, Kattner G, Kuosa H, et al. 2014. Physical and bacterial controls on inorganic nutrients and dissolved organic carbon during a sea ice growth and decay experiment. *Mar Chem* **166**: 59–69. doi: 10.1016/j.marchem.2014.09.013.

Contributions

- Contributed to conception and design: SM, HK, BD, MK
- Lead of the INTERICE V experiment: DT
- Contributed to planning and experimental design of INTERICE V: DT, HK, GD, J-LT, BD
- Contributed to carry out the experiment and acquisition of data: JZ, GD, DT, J-LT, BD
- Contributed to analysis and interpretation of data: SM, HK, BD, MK
- Contributed to the modelling analysis: SM, MV
- Drafted and/or revised the article: SM with early interactions with BD and HK and with comments and inputs from all coauthors
- Final approval of the version to be published: all co-authors

Acknowledgments

The authors would like to thank the others in the Interice V team and the crew of the Hamburg Ship Model Basin (HSVA), especially Karl-Ulrich Evers, for their hospitality, technical and scientific support and the professional execution of the test program in the Research Infrastructure Arctic Technology Laboratories (ARCTECLAB). We also thank the Scientific Committee on Ocean Research (SCOR) working group 140 on Biogeochemical Exchange Processes at the Sea Ice Interfaces (BEPSII) for setting the ground for discussions and building projects among the sea ice biogeochemistry community.

Funding information

The work described in this publication was supported by the Belgian Science Federal Policy Office (BIGSOUTH project) and by the European Community's 7th Framework Program through the grant to the budget of the Integrated Infrastructure Initiative HYDRALAB-IV, Contract no. 261520 and the BISICLO project (FP7 CIG 321938). DT and HK received funding through the Academy of Finland (Finland Distinguished Professor Programme, project 127097) and the Walter and Andrée de Nottbeck Foundation. MK, JZ, SM and BD are respectively research fellows, a postdoctoral researcher and a research associate of the Fonds de la Recherche Scientifique - FNRS. JZ is a BAEF-Francqui Foundation Research Fellow. This is a Mare contribution 311.

Competing interests

The authors have declared that no competing interests exist.

Data accessibility statement

The observation data and the model code will be made available to any scientist upon request. We encourage other scientists to use our code in order to reproduce and test the model results in other locations (contacts: s.moreau@uclouvain.be and bruno.delille@ulg.ac.be).